

Early to late spectroscopic and photometric analysis of the type IIb SN 2013df

A. Morales-Garoffolo¹, N. Elias-Rosa², and J. Isern¹

¹ Institut de Ciències de l'Espai (CSIC-IEEC), Campus UAB, Torre C5, 2a planta, 08193 Barcelona, Spain

² INAF Osservatorio Astronomico di Padova, Vicolo dell'Osservatorio 5, 35122 Padova, Italy

Abstract

We present the summary of the analysis of the optical observational data of the type IIb SN 2013df from a few days to about 250 days after explosion. SN 2013df presents a double-peak optical light curve that is similar to those of SNe 1993J and 2011fu although with different decline and rise rates. From the modelling of the pseudo-bolometric light curve, which includes UV data taken by *SWIFT*, we have estimated a total mass of synthesised ⁵⁶Ni in the explosion of $\sim 0.1 M_{\odot}$, while the ejecta mass is $0.8\text{--}1.4 M_{\odot}$, and the explosion energy $0.4\text{--}1.2 \times 10^{51}$ erg. In addition, we have estimated a lower limit to the progenitor radius ranging from $64 - 169 R_{\odot}$ and the spectral evolution indicates that SN 2013df had a hydrogen envelope similar to SN 1993J ($\sim 0.2 M_{\odot}$). The line profiles in nebular spectra suggest that the explosion was asymmetric with the presence of clumps in the ejecta, while the [O I] $\lambda\lambda 6300, 6364$ luminosities, may indicate that the progenitor of SN 2013df was a relatively low mass star ($\sim 12 - 13 M_{\odot}$).

1 Introduction

Massive stars ($M_{ZAMS} > 8 M_{\odot}$; see e.g., [9]) usually end their lives exploding as Core-Collapse Supernovae (CC-SNe) leaving behind a compact remnant (neutron star or black hole depending on the mass of the star that exploded). The stellar configuration prior to explosion is what leads to the different observational sub types of CC-SNe. Specifically, type IIb SNe are thought to arise from the explosion of stars that had retained a small part (a few tenths of M_{\odot}) of their hydrogen layer, and along with type Ib and Ic SNe belong to the so-called stripped-envelope SNe category [6]. The reason why type IIb SN progenitors have lost most of their hydrogen envelope prior to exploding is unclear, although two scenarios are contemplated: 1) Transfer of most of the stellar envelope of the progenitor to a companion star

(see e.g. [5]); 2) Mass loss due to stellar winds [20, 16] Type IIb SNe are relatively infrequent events. Their rate among a volume limited sample of 81 type II SNe was estimated by [12] to be $11.9\%_{-3.6}^{+3.9}$. Additionally, the Asiago SN catalogue lists about 86 type IIb SNe¹ but only a few of them have been extensively monitored. The main characteristic of this subtype of SNe is the transition showed in their spectra from being dominated by hydrogen at early phases, to predominance of He I features at later times [7]. Concerning their light curves (LCs), some type IIb SNe present clear double-peaked LCs in all optical bands, as in the case of SN 1993J (see e.g. [17]) and SN 2011fu [11]. Other IIb SNe show the first peak only in some of their optical and UV bands, e.g. SNe 2008ax [18] and 2011dh [1]. This is probably due to the short duration of the first peak in these SNe that can be missed by observations.

SN 2013df, having coordinates $\alpha = 12^{\text{h}}26^{\text{m}}29^{\text{s}}.33$ and $\delta = +31^{\circ}13'38.''3$ (J2000), was discovered in the galaxy NGC 4414 by F. Ciabattari and E. Mazzoni of the Italian Supernovae Project (ISSP)², on 2013 June 7.87 UT [4]. A spectrum of SN 2013df taken soon after discovery (2013 June 10.8 UT) showed characteristics of a type II supernova resembling early spectra of the type IIb SN 1993J [4]. The analysis of Hubble Space Telescope (HST) archival images led to the detection of the probable yellow supergiant progenitor of the supernova, the results are presented in [24] together with some early time SN data. Here we present the most important results of the analysis of our optical photometric and spectroscopic follow-up data for SN 2013df spanning from a few days up to 250 days after explosion (see [14] for details of the instrumental set-ups used in the acquisition of our data of SN 2013df, as well as the data reduction process and the detailed analysis of the complete data set). The distance modulus and recession velocity of the SN as well as the reddening in its line of site, and the explosion epoch adopted throughout this work are summarized in Table 1, (see also [14] for more details). The monitoring of SN 2013df from early to late time after explosion, has offered us a unique opportunity to investigate the evolution of the observed properties of a relatively nearby double-peaked type IIb SN, and for which the plausible progenitor has been identified.

2 Photometric Results

SN 2013df was observed in the optical *UBVRI* and ultraviolet *UVW2*, *UVM2*, *UVW1* bands. Since we do not have NIR data we assumed a NIR contribution to the pseudo-bolometric LC equal to that of SN 1993J. In the left panel of Fig. 1 we present the comparison of the computed optical-NIR pseudo-bolometric light curves of several type IIb SNe with that of SN 2013df. The overall shape of the LC of SN 2013df is similar to those of SNe 1993J and 2011fu since it presents two peaks. The first peak of the LCs of IIb SNe is attributed to shock wave heating of the hydrogen envelope of the progenitor star, while the longer lasting secondary peak is powered by the decay of ^{56}Ni [25]. As can be seen in the figure, SN 2013df has a slower cooling phase after the first peak than SN 1993J. The secondary peak luminosity of SN 2013df lies between those of SN 2011dh and SN 1993J, while the LC width seems smaller following standard light curve interpretation [2]. This suggests that the ejected ^{56}Ni mass of

¹<http://sngroup.oapd.inaf.it>

²<http://italiansupernovae.org/en.html>

SN 2013df should lie between those of SNe 2011dh and 1993J while the ejecta mass should be lower than for those two SNe. At late phases, the LC tail follows the trend of SN 1993J although the slope is a bit steeper and this again could indicate a lower ejecta mass than for SN 1993J. In order to derive the explosion parameters of SN 2013df, we have modelled the bolometric light curve as described in [23], the results of which are presented in Table 1. The derived ^{56}Ni and ejecta masses are consistent with the comparison to other type IIb SNe (see also Table 7 of [14]). In the left panel of Fig. 1 we have represented the UV-optical-NIR pseudo-bolometric LC of SN 2013df together with its best fitting model.

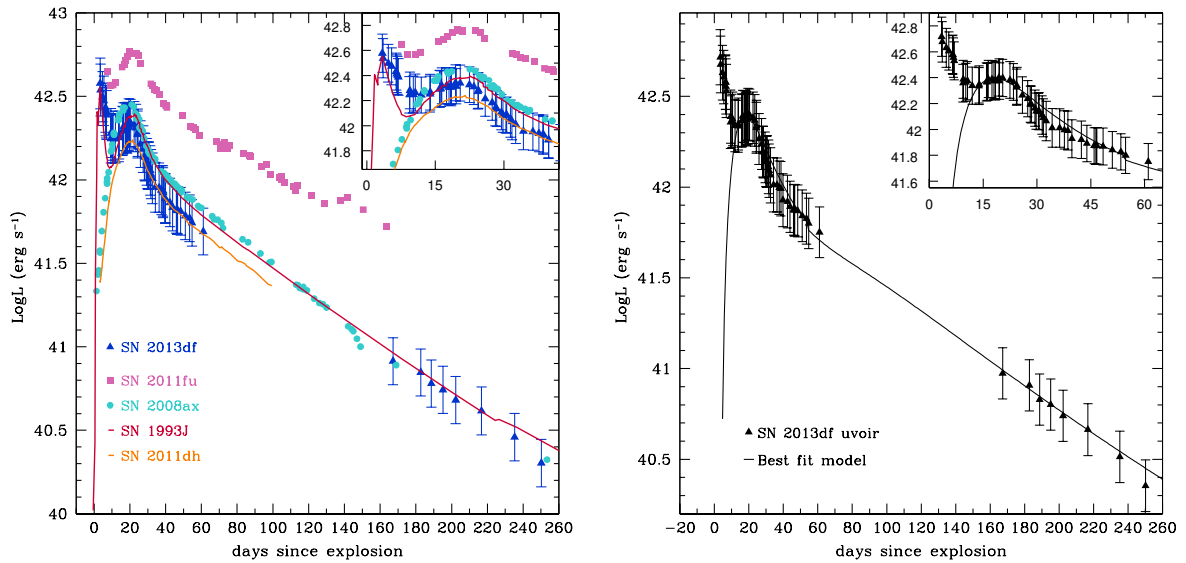


Figure 1: Left panel: Pseudo-bolometric optical-NIR LC of SN 2013df compared to those of other type IIb SNe. Right panel: Pseudo-bolometric UV-optical-NIR LC of SN 2013df compared to its best fit model. For clarity, we have zoomed in on the light curves up to phase ~ 40 d in the upper right corner of the panels.

Table 1: Adopted characteristics and derived explosion parameters of SN 2013df.

Explosion epoch (+2400000)	μ (mag)	Rec.Velocity (km s^{-1})	$E(B-V)$ (mag)	E_{kin} (10^{51}erg)	^{56}Ni mass (M_{\odot})	M_{ej} (M_{\odot})
56450.0 ± 0.9	31.65 ± 0.30	716 ± 6	0.10 ± 0.02	$0.4 - 1.2$	$0.10 - 0.13$	$0.8 - 1.4$

3 Spectroscopic Results

Our spectral sequence of SN 2013df covers the evolution from 9 up to 243 days post explosion, with a seasonal visibility gap between 42 and 183 days. It is shown in Fig. 2 together with the identification of the most prominent lines. In the spectrum at 9 days (that is near the

minimum after the first peak in the LCs), we identify a clear P-Cygni $H\alpha$ feature and an absorption component of $H\beta$ at around 4700 \AA . Both the absorption components of $H\alpha$ and $H\beta$ exhibit a flat-bottom profile indicating the presence of a thick expanding H shell [3]. The spectrum at 42 days presents a significant decrease in flux at blue wavelengths compared to earlier data. The $H\alpha$ line diminished by a factor of 4 approximately, while He I lines increased in intensity with respect to the preceding spectra by a factor of 1.3 approximately. Furthermore, the He I features at $\lambda 6678$ and $\lambda 7065$ respectively, can be identified in this spectrum [22, 8] while they were absent in the previous spectra. The last two spectra of our sequence, taken at phases of 183 and 243 days after explosion, exhibit a relative increase in flux at blue wavelengths as well as strong lines of [O I] $\lambda\lambda 6300, 6364$, [Ca II] $\lambda\lambda 7291, 7324$, O I $\lambda 7774$, and Ca II NIR. We also identify Na I around 5890 \AA possibly contaminated by residual He I $\lambda 5876$, and Fe II around 5000 \AA [22, 13, 19]. We believe the features around $6500\text{-}6600 \text{ \AA}$ and $6700\text{-}6800 \text{ \AA}$ might be associated to $H\alpha$ emission emerging after asymmetric ejecta-circumstellar material interaction (see [21]). Overall we find SN 2013df's spectra most similar to those of SN 1993J at coeval phases (see Fig. of [14]), this is specially so for the hydrogen lines.

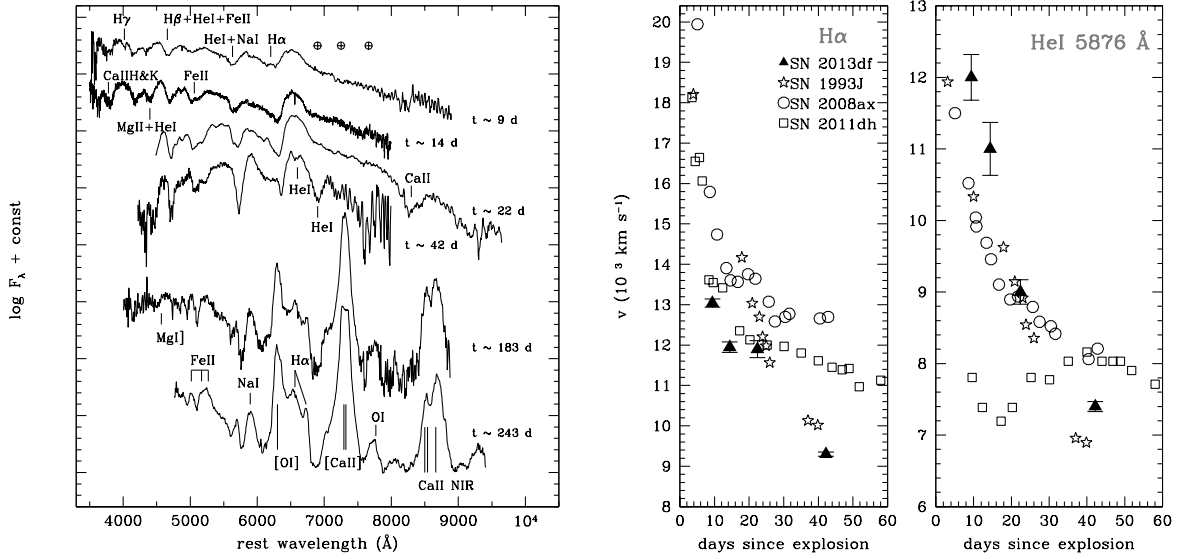


Figure 2: Left panel: Optical spectral evolution of SN 2013df, where the most relevant features in the spectra are indicated. Telluric features have been marked with \oplus . The spectra have been corrected for the host galaxy redshift. Epochs indicated in the plot are with respect to our assumed explosion date of $\text{JD} = 2456450.0 \pm 0.9$. Spectra have been shifted vertically for clarity. Right panel: Early evolution of the velocities of $H\alpha$ and He I $\lambda 5876$ for IIb SNe 2013df, 1993J and 2008ax and 2011dh.

In the right panel of Fig. 2 we show the evolution of the expansion velocities of $H\alpha$ and He I $\lambda 5876$, derived from the positions of the minima of the P-Cygni absorptions, for SNe 2013df, 1993J, 2008ax, and 2011dh. These velocities give an idea of the velocities of the

shells where the lines are forming. As can be seen in the figure, there is an overall similar trend among the different SNe. Although the $H\alpha$ velocities are somewhat lower than for the rest of the SNe, while the $\text{He I } \lambda 5876$ velocities seem to exhibit higher values and a steeper gradient.

An analysis of the profiles in the nebular spectra of the SN has permitted us on one hand distinguish some substructure (due to clumping in the ejecta) underlying the global components of the $[\text{O I}] \lambda\lambda 6300, 6364$ and $[\text{Ca II}] \lambda\lambda 7291, 7324$ lines (see Fig. 10 of [14]). On the other hand, the luminosities we derived from the $[\text{O I}] \lambda\lambda 6300, 6364$ line in our nebular spectra are consistent with those of progenitors with $M_{\text{ZAMS}} 12M_{\odot}$ and $13M_{\odot}$ [10].

4 Further constraints on the progenitor

Although the ideal way to set additional constraints on the progenitor of SN 2013df would be through hydrodynamical modelling of the LC including the early peak, we have attempted to do this by following the analytical prescription of [15]. According to this, the luminosity at first peak gives the extended radius of the progenitor, from the time of the first peak the extended mass around the extended radius may be derived, and the time of the minimum after first peak leads to an estimate of an upper limit to the core mass of the progenitor. In summary, we obtained that the extended radius of the progenitor of SN 2013df should have been at least $64 - 169 R_{\odot}$. While the extended mass around the extended radius results similar to that of SN 1993J ($0.05 - 0.09 M_{\odot}$). And the upper limit to the core radius results $45 - 238 \cdot 10^{11}$ cm, which is larger than those of SNe 1993J and 2011dh (that are in the range $5 - 9 \cdot 10^{11}$ cm).

5 Summary

According to the analysis of our observations, the star that exploded as SN 2013df had an extended radius greater than $64 - 169 R_{\odot}$, an extended hydrogen envelope whose mass was probably similar to that of SN 1993J ($M_{\text{H}} \sim 0.2 M_{\odot}$), and a M_{ZAMS} possibly around $12M_{\odot}$ - $13M_{\odot}$. In the explosion, approximately $0.8-1.4 M_{\odot}$ was ejected with a kinetic energy of $0.4-1.2 \times 10^{51}$ erg, in addition to $\sim 0.1 M_{\odot}$ of ^{56}Ni being synthesised. According to our spectra, the ejecta is possibly distributed in clumps and has plausibly suffered some interaction with pre-explosion circumstellar material around the progenitor.

SN 2013df is the third type IIb SN presenting double-peaked light curves in all its optical bands. In addition, its progenitor has been identified in archival images. Our analysis of the dataset of SN 2013df hopefully contributes to the characterization of the relatively rare type IIb CC-SNe subclass.

Acknowledgements

We would like to thank the following people who have contributed to this work with observations and important feedback: S. Benetti, S. Taubenberger, E. Cappellaro, A. Pastorello, M. Klauser, S.

Valenti, S. Howerton, P. Ochner, N. Schramm, A. Siviero, L. Tartaglia, L. Tomasella, A. Jerkstrand, and A. Serenelli. A.M.G. acknowledges financial support by the Spanish *Ministerio de Economía y competitividad* (MINECO) grant ESP2013-41268-R. N.E.R. acknowledges the support from the European Union Seventh Framework Programme (FP7/2007-2013) under grant agreement n. 267251 “Astronomy Fellowships in Italy” (AstroFit). J.I. acknowledges support by the Spanish *Ministerio de Economía y competitividad* (MINECO) grant ESP2013-47637-P.

References

- [1] Arcavi I., Gal-Yam A., Kasliwal M. M., et al. 2011, *ApJL*, 742, L18
- [2] Arnett W. D., 1982, *ApJ*, 253, 785
- [3] Barbon R., Benetti S., Cappellaro E., et al. 1995, *A&AS*, 110, 513
- [4] Ciabattari F., Mazzoni E., Donati S., et al. 2013, *Cent. Bur. Electr. Telegram*, 3557, 1
- [5] Claeys J. S. W., de Mink S. E., Pols O. R., Eldridge J. J., Baes M., 2011, *A&A*, 528, A131
- [6] Clocchiatti A., Wheeler J. C., Benetti S., Frueh M., 1996, *ApJ*, 459, 547
- [7] Filippenko A. V., 1988, *AJ*, 96, 1941
- [8] Hachinger S., Mazzali P. A., Taubenberger S., et al. 2012, *MNRAS*, 422, 70
- [9] Heger A., Fryer C. L., Woosley S. E., Langer N., Hartmann D. H., 2003, *ApJ*, 591, 288
- [10] Jerkstrand A., Ergon M., Smartt S. J., et al. 2014, preprint (arXiv:1408.0732v1)
- [11] Kumar B., Pandey S. B., Sahu D. K, et al. 2013, *MNRAS*, 431, 308
- [12] Li W., Leaman J., Chornock R., et al. 2011, *MNRAS*, 412, 1441
- [13] Matheson T., Filippenko A. V., Barth A. J., et al. 2000, *AJ*, 120, 1487
- [14] Morales-Garoffolo A., Elias-Rosa N., Benetti S., et al. 2014, *MNRAS*, 445, 1647
- [15] Nakar E. & Piro A. L., 2014, *ApJ*, 788, 193
- [16] Puls J., Vink J. S., Najarro F., 2008, *A&AR*, 16, 209
- [17] Richmond M. W., Treffers R. R., Filippenko A. V., et al. 1994, *AJ*, 107, 1022
- [18] Roming P. W. A., Pritchard T. A., Brown P. J., et al. 2009, *ApJ*, 704, L118
- [19] Shivvers I., Mazzali P., Silverman J. M., et al. 2013, *MNRAS*, 436, 3614
- [20] Smith, N. & Owocki S. P., 2006, *ApJL*, 645, L45
- [21] Smith N., Cenko S. B., Butler N., et al. 2012, *MNRAS*, 420, 1135
- [22] Taubenberger S., Navasardyan H., Maurer J. I, et al. 2011, *MNRAS*, 413, 2140
- [23] Valenti S., Benetti S., Cappellaro E., et al. 2008, *MNRAS*, 383, 1485
- [24] Van Dyk S. D., Zheng W., Fox O. D, et al. 2014, *AJ*, 147, 37
- [25] Woosley S. E., Eastman R. G., Weaver T. A., Pinto P. A., 1994, *ApJ*, 429, 300